sarily mean a major shift in water mass boundaries in subtropical latitudes. Only in the case of shell porosity does a discontinuity exist in the morphologic gradient between the two cluster groups. This is evident from Fig. 2a, where shell porosity is plotted against shell diameter for the sediment samples. These data show that all samples in the central water mass fall along a line with a different slope from the line representing those in the equatorial waters. Thus, the gradient in one of these morphologic parameters must be discontinuous between the two water masses; in Fig. 2, b and c, shell porosity and shell diameter are plotted against water density. Variations in shell diameter are clearly gradational between the two water masses, but variations in shell porosity are discontinuous (*9*). All equatorial samples are drawn from waters of similar density, but show a wide range of variation in shell porosity. Central water mass samples, on the other hand, show a narrow range of porosity variation over wide changes in water density (*10*). Thus, shell porosity is a critical morphologic index whose geographic variation probably reflects fundamental ecologic differences between *O. universa* populations in the equatorial and central water masses.

The discontinuity in morphologic gradient in populations of *O. universa* provides an important paleoclimatic index. Its value may be in providing an independent check on proposed paleoclimatic reconstructions. McIntyre *et al.* (*3*) recently compared August temperatures in the Indian Ocean today and 18,000 years before present (B.P.) as derived from faunal paleotemperature estimates. The morphologic boundary between the equatorial and central water masses today parallels the August 24°C isotherm. This isotherm, computed for the time of the last major ice age (18,000 years B.P.), is essentially in the same position as today, indicating that no major displacement in water masses had occurred in this region. Independent verification of this paleoclimatic reconstruction may be derived from analysis of morphologic gradients in populations of *O. universa* from this region.

ALAN D. HECHT*
Department of Geology,
West Georgia College,
Carrollton 30117

ALLAN W. H. BÉ
LEROY LOTT
CLIMAP, Columbia University,
Lamont-Doherty
Geological Observatory,
Palisades, New York 10964

References and Notes

1. J. Imbrie and N. Kipp, in *The Late Cenozoic Glacial Ages*, K. K. Turekian, Ed. (Yale Univ. Press, New Haven, Conn., 1971), p. 71.
2. W. F. Ruddiman and L. K. Glover, *Quat. Res. (N.Y.)* **5**, 361 (1975); A. W. H. Bé and J. C. Duplessy, *Science* **194**, 419 (1976).
3. A. McIntyre *et al.*, *Science* **191**, 1131 (1976).
4. A. W. H. Bé, S. M. Harrison, L. Lott, *Micropaleontology* **19** (No. 2), 150 (1973).
5. G. H. Scott [in *Foraminifera*, R. H. Hedley and G. G. Adams, Eds. (Academic Press, London, 1974), vol. 1, p. 55] recently reviewed the multivariate statistical analyses (cluster, factor, and ordination methods) that can be used to objectively define morphologic groups. However, each of these methods, because of its mathematical assumptions, tends to produce different groupings of samples. In fact, various strategies within each method also tend to produce different geographic groupings. Pritchard and Anderson (*6*), for example, showed that a single data set (floral data in this case), when analyzed by six different clustering strategies (single linkage, group average, complete linkage, centroid, median, and minimum variance), produced different geographical groupings of their samples. However, from their data an optimum strategy for defining morphologic groups can be formulated. For example, of the six intracluster strategies listed above, the optimum method for formulating morphologic groups appears to be clustering by either group average, complete linkage, or minimum variance. For each of these methods, the resulting dendrograms are the same and show sharp cluster breaks from which morphologic provinces can be determined. The dendrograms resulting from centroid, median, and single linkage clusters are also nearly the same, but tend to produce dendrograms without sharp boundaries. The computer program used in this analysis is that of Pritchard and Anderson.
6. N. M. Pritchard and A. J. B. Anderson, *J. Ecol.* **59**, 727 (1971).
7. R. R. Sokal and P. H. A. Sneath, *Numerical Taxonomy* (Freeman, San Francisco, ed. 2, 1973).
8. K. Wyrtki, in *The Biology of the Indian Ocean*, B. Zeitzschel, Ed. (Springer-Verlag, New York, 1973), p. 18; *Oceanographic Atlas of the International Indian Ocean Expedition* (National Science Foundation, Washington, D.C., 1971), p. 71.
9. A. W. H. Bé, S. M. Harrison, W. E. Frerichs, M. E. Heiman, in *Progress in Micropaleontology*, Y. Takayanagi and T. Saito, Eds. (Micropaleontology Press, New York, 1976), p. 1.
10. Similar results are obtained for plots of shell porosity and shell diameter against surface temperature.
11. We thank M. Bohn and K. Roddenberry for assistance in the computer analysis. A.D.H. received support from NSF grant GA-43244 and A.W.H.B. from NSF grants 75-21366, 75-19627, and 76-02202. Most of the sediment cores used in the study are from the Lamont-Doherty Geological Observatory Core Library, which is maintained by grants from the Office of Naval Research (NOOO 14-75-C-0210) and the National Science Foundation (DES 72-01568A04). A few cores were obtained from Scripps Institution of Oceanography and Woods Hole Oceanographic Institution. Lamont-Doherty Geological Observatory Contribution No. 2394.
* Present address: Climate Dynamics Research Section, Division of Atmospheric Sciences, National Science Foundation, Washington, D.C. 20550.

18 March 1976; revised 23 July 1976

Activating Factor for the Iron Protein of Nitrogenase from *Rhodospirillum rubrum*

Abstract. *As isolated from* Rhodospirillum rubrum, *the iron protein of nitrogenase has little or no activity. It can be activated by incubating it with a trypsin-sensitive, oxygen-labile component (activating factor) plus adenosine triphosphate and a divalent metal ion. After activation, the iron protein retains its nitrogenase activity when the activating factor is removed.*

Although the molybdenum-iron protein of *Rhodospirillum rubrum* nitrogenase has been partially purified (*1*), little success in purifying the iron protein has been reported. However, several observations have indicated that the *R. rubrum* nitrogenase system differs from nitrogenase in other bacteria; chromatophores (membrane fragments containing the photosynthetic apparatus) strongly inhibit nitrogenase activity in crude extracts, and a high level of $MgCl_2$ (25 m*M*) is optimal for the assay of nitrogenase in the presence of only 5 m*M* adenosine triphosphate (ATP) (*2*). The time course of reductions catalyzed by *R. rubrum* nitrogenase is nonlinear, and a lag phase of 10 to 15 minutes is common (*3*). Our discovery of an activating factor (AF) for

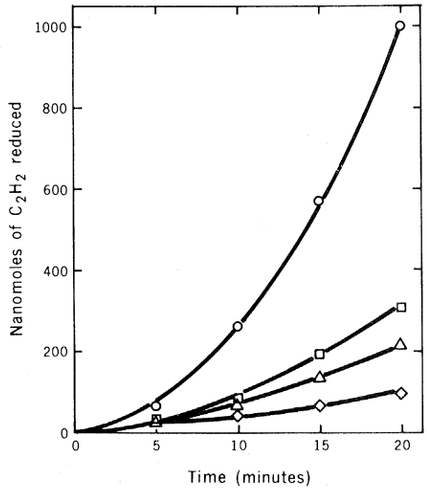

Fig. 1. Assays were performed in 21-ml vaccine bottles at 30°C. Total volume of the reaction mixture was 1 ml; it contained 5 m*M* ATP, 30 m*M* creatine phosphate, 0.05 mg of creatine phosphokinase, 0.4 ml of crude extract which had a protein concentration of 8.4 mg/ml, 10 m*M* $Na_2S_2O_4$, and 40 m*M* triethanolamine-acetate buffer. The gas phase was 90 percent H_2 and 10 percent C_2H_2. C_2H_4 was measured by gas chromatography. ○——○, 25 m*M* Mg^{2+} and 0.5 m*M* Mn^{2+}; □——□, 10 m*M* Mg^{2+} and 0.5 m*M* Mn^{2+}; △——△, 25 m*M* Mg^{2+}; ◇——◇, 10 m*M* Mg^{2+}.

Table 1. Separation of activating factor from anaerobically collected chromatophores. Assays were performed as described in Fig. 1 legend with 25 m*M* $MgCl_2$ and 0.5 m*M* $MnCl_2$ added. Chromatophores were sedimented by centrifugation at 45,000*g* for 2 hours; supernatant is referred to as crude extract. Chromatophores from 100 ml of extract were resuspended in 30 ml of 50 m*M* triethanolamine buffer (*p*H 7.5). Resuspended chromatophores were centrifuged for 1 hour at 45,000*g*; the supernatant fluid was the buffer wash. Chromatophores were resuspended in 30 ml of 0.5*M* NaCl in buffer and again were centrifuged at 45,000*g* for 1 hour to yield the salt wash and final chromatophores; 0.2 ml of crude extract or other fraction was added where indicated.

Components of reaction mixture	C_2H_2 reduced (nmole) per 20 minutes
Crude extract	588
Crude extract plus resuspended chromatophores	2100
Crude extract plus buffer wash from chromatophores	1008
Crude extract plus salt wash from chromatophores	2436
Crude extract plus final chromatophores	798
Resuspended chromatophores	210
Final chromatophores	0
Buffer wash	54
Salt wash	0

the Fe protein of *R. rubrum* nitrogenase explains these unusual responses.

Cells of *R. rubrum* (ATCC 11170) were grown anaerobically in the light on Ormerod's medium (*4*) to an absorbance of 0.7 at 650 nm. Cells grown on glutamate produce nitrogenase. The cells were collected under N_2 and all manipulations were made under N_2. This is critical, because chromatophores from aerobically collected cells inhibit the enzyme, whereas chromatophores from cells collected under N_2 increase activity as much as fivefold. The cells were broken by osmotic shock (glycerol) and chromatophores containing the AF were recovered by centrifugation.

A marked enhancement by low concentrations of Mn^{2+} was observed in an experiment in which the requirement for high concentrations of Mg^{2+} was verified (Fig. 1). In contrast, no additive effects have been found with any combination of metal ions in the *Azotobacter* system (*5*), although Mn^{2+} substitutes partially for Mg^{2+}.

The observations with Mg^{2+} and Mn^{2+} led to the discovery that the brown protein eluted from a diethylaminoethyl (DEAE) cellulose column, and assumed to be the Fe protein, (i) could be activated by the addition of a small amount of crude extract, (ii) that AF could be separated from the MoFe and Fe proteins on a DEAE cellulose column, and finally (iii) that more AF could be eluted from chromatophores of anaerobically collected cells than could be recovered from the supernatant fraction (Table 1). The AF has been isolated from cells grown on either glutamate or NH_4Cl. Cells grown in the presence of excess NH_4^+ produce no active MoFe or Fe proteins.

It was possible to prepare an active Fe protein and to separate the AF from it on a DEAE cellulose column. After the activation, there no longer was enhancement of activity by excess Mg^{2+} or Mn^{2+} and the C_2H_2 reducing activity of the Fe protein was linear with time (Fig. 2). The AF activity also was recovered from the column.

The data of Table 2 demonstrate the functioning of three components for both C_2H_2 reduction and N_2 reduction. The activating factor was eluted from washed chromatophores (see Table 1) and then precipitated with 30 percent polyethylene glycol 4000. The AF was redissolved in buffer, loaded onto a DEAE column, and eluted with 100 m*M* NaCl. The highest specific activity obtained for Fe protein was 1215 nmole of C_2H_2 reduced in 1 minute per milligram of protein.

The MoFe protein from *R. rubrum* will cross react with the Fe protein from *Azotobacter vinelandii* to yield an active nitrogenase, and activity of the MoFe protein during its purification can be followed with the Fe protein from *A. vinelandii*. There is no indication that AF has any effect on the MoFe protein.

Despite the requirement of ATP for activation, the Fe protein is not adenylated during activation, nor is ^{32}P from [γ-^{32}P]ATP incorporated into the Fe protein during activation. No new protein band detectable on polyacrylamide gels is generated during activation.

Although the AF from *R. rubrum* has no obvious similarities to previously described putative third components in other nitrogenase systems (*6*), it is interesting to note (*7*) that Fe^{2+} and ATP have been used to reactivate bacteroid extracts that have lost activity. The reactions have been thought to be nonspecific, but it is possible that an AF system similar to that in *R. rubrum* has been involved.

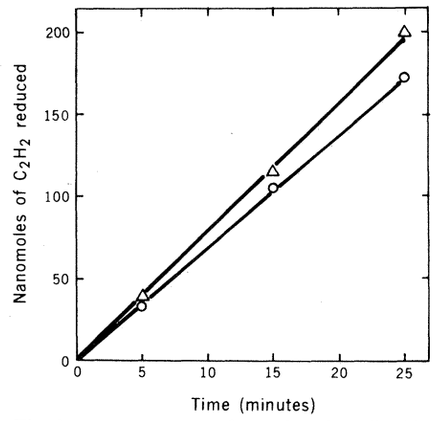

Fig. 2. Assays were performed as described in Fig. 1 legend. Fe protein was activated for 50 minutes at 30°C in a mixture containing 5 m*M* ATP, 30 m*M* creatine phosphate, 0.05 mg of creatine phosphokinase, 25 m*M* $MgCl_2$, 0.2 m*M* $MnCl_2$, 1 m*M* $Na_2S_2O_4$, 3.5 ml of Fe protein, and 2.0 ml of AF in a total volume of 10 ml. After incubation the mixture was placed on a DEAE cellulose column. Activating factor was eluted with 150 m*M* sodium malate (*p*H 7.5), and activated Fe protein was eluted with 400 m*M* sodium malate. Fifty microliters of activated Fe protein were assayed together with 5 μl of MoFe protein. △——△, 10 m*M* Mg^{2+}; ○——○, 25 m*M* Mg^{2+} and 0.2 m*M* Mn^{2+}.

Only in *Clostridium pasteurianum*, *A. vinelandii*, *Azotobacter chroococcum*, and *Klebsiella pneumoniae* have two and only two nitrogenase components been purified to homogeneity and shown to be sufficient for enzymatic activity. The possibility should be investigated that an activating component is present and functions in other nitrogen-fixing organisms, especially the photosynthetic organisms. Two criteria useful in determining whether an organism has a nitrogenase system

Table 2. Requirement for a third factor to convert the Fe protein of *R. rubrum* to a form catalytically active in the reduction of N_2 and C_2H_2. Assays were done as described in Fig. 1 legend except that N_2 reductions were under 1 atm of N_2; the reaction mixture contained 280 μg of Fe protein, 600 μg of MoFe protein, and 105 μg of AF. Ammonia was determined by the "indophenol method" after microdiffusion (*8*).

Components of reaction mixture (*9*)	Nanomoles of C_2H_2 reduced during				Nanomoles of N_2 reduced (20 minutes)
	5 minutes	10 minutes	15 minutes	20 minutes	
Complete	60	270	585	915	166
Without Fe protein	0	0	0	0	13
Without AF	0	0	0	0	12
Without MoFe protein	0	0	0	0	12

like that of *R. rubrum* are nonlinearity of the time course of substrate reduction and enhancement of activity by 0.5 m*M* Mn^{2+}.

PAUL W. LUDDEN, R. H. BURRIS
Department of Biochemistry, University of Wisconsin–Madison, Madison 53706

References and Notes

1. D. R. Biggins, M. Kelly, J. R. Postgate, *Eur. J. Biochem.* **20**, 140 (1971).
2. R. C. Burns and W. A. Bulen, *Arch. Biochem. Biophys.* **113**, 461 (1966).
3. T. O. Munson and R. H. Burris, *J. Bacteriol.* **97**, 1093 (1969).
4. S. K. Bose, in *Bacterial Photosynthesis*, H. Gest, Ed. (Antioch Press, Yellow Springs, Ohio, 1963), p. 502.
5. R. C. Burns, *Biochim. Biophys. Acta* **171**, 253 (1969).
6. L. E. Mortenson, *ibid.* **127**, 18 (1966); K. B. Taylor, *J. Biol. Chem.* **244**, 171 (1969); S. Kajiyama, T. Matsuki, Y. Nosoh, *Biochem. Biophys. Res. Commun.* **37**, 711 (1969).
7. F. J. Bergersen and G. L. Turner, *Biochem. J.* **131**, 61 (1973); I. R. Kennedy, J. Riguad, J. C. Trinchant, *Biochim. Biophys. Acta* **397**, 24 (1975).
8. R. H. Burris, in *Methods Enzymol.* **24B**, 415 (1972).
9. The MoFe protein was purified by elution from a DEAE column with 150 m*M* malate at *p*H 7.5 in 50 m*M* triethanolamine (TEA) buffer followed by another DEAE column from which the MoFe protein was eluted by malate in a gradient from 0 to 400 m*M*. The Fe protein was eluted from the first DEAE column with 450 m*M* NaCl in 50 m*M* TEA buffer and then was diluted with buffer before being concentrated on a second DEAE column. The concentrated Fe protein was purified further by preparative gel electrophoresis.
10. Supported by the College of Agricultural and Life Sciences, University of Wisconsin–Madison, by PHS grant AI-00848, and by NSF grant PCN74-17604.

5 April 1976; revised 14 June 1976

Reinnervation of Dentate Gyrus by Homologous Afferents Following Entorhinal Cortical Lesions in Adult Rats

Abstract. *Granule cells of the rat dentate gyrus which are denervated by unilateral destruction of the entorhinal cortex are reinnervated in part by proliferation of surviving pathways from the contralateral entorhinal cortex. The cells of origin of these lesion-induced projections were identified by retrograde labeling with horseradish peroxidase and were the same cell type which normally project to the ipsilateral dentate gyrus.*

Cells of the mature brain that are deprived of their normal synaptic input as a consequence of lesions can, in some cases, be reinnervated by nearby afferent systems which sprout new synaptic connections (*1*). The functional significance of such reinnervation has been difficult to ascertain, often because the relationship between the cells which were destroyed by the lesion and those providing the new synaptic connections is unclear. The hippocampal formation of the rat, however, provides a situation in which comparisons between normal and lesion-induced circuitry are possible.

Unilateral lesions of the entorhinal area (Broadman's area 28), which gives rise to the major extrinsic afferent nerves to the dentate granule cells of the ipsilateral hippocampal formation (*2*), apparently induce proliferation of several surviving afferents in the dentate gyrus, resulting in extensive reinnervation of the dentate granule cells (*3, 4*). Among the areas that give rise to fibers which reinnervate the granule cells is the surviving contralateral entorhinal cortex (*4*). While this area normally sends only a very sparse crossed projection to the contralateral dentate gyrus (*5, 6*), these crossed temporo-dentate projections proliferate by 500 to 600 percent in response to unilateral entorhinal lesions (*6*).

The reinnervation of the dentate granule cells by afferents of contralateral entorhinal origin clearly results in the reestablishment of a pathway which is similar in many respects to the ipsilateral circuitry that was destroyed by the lesion. First, the reinnervating fibers terminate in a topographically organized fashion which resembles the normal pattern of ipsilateral entorhinal innervation (*7*). Second, the crossed projections exhibit many of the physiological properties of the normal ipsilateral circuitry (*6*). Third, since the surviving entorhinal area is the contralateral homolog of the damaged region, the reinnervating afferents might well be anatomically homologous with the normal ipsilateral circuitry. Yet the most critical issue in evaluating homology is not whether the lesion-induced circuitry arises from a homologous cortical area, but rather whether it arises from the same cell types within the cortical area as the normal circuitry. To investigate this question, use was made of the retrograde transport of horseradish peroxidase (HRP) to identify the cells of origin of the normal ipsilateral and the lesion-induced crossed temporo-dentate circuitry.

A total of 14 male Sprague-Dawley rats served as experimental animals. The entorhinal cortical region was unilaterally ablated as described previously (*3, 4*). After the operation, the animals were allowed to recover for 9 to 12 months before being injected with HRP. A 30 to 50 percent solution of HRP (Sigma type VI) in distilled water was injected into the dentate gyrus which had been deprived of ipsilateral entorhinal input and subsequently reinnervated by the contralateral entorhinal cortex. Injection volumes ranged from 0.3 to 0.4 μl and were delivered over a period of 30 to 45 minutes. Forty-eight hours after injection, the animals were deeply anesthetized with sodium pentobarbital and perfused transcardially with 10 percent formalin-saline. The brains were removed, fixed for 2 to 3 hours in the perfusion solution at 5°C, and then sectioned in the horizontal plane. Sections were incubated in tris buffer (*p*H 7.4) containing 3,3′-diaminobenzidine and hydrogen peroxide, according to histochemical methods described elsewhere (*8*). The brown product that results from this histochemical reaction can best be viewed with dark-field illumination where HRP-positive granules appear greenish yellow (see Fig. 1). For the purpose of comparison with normal animals, illustrative material was drawn from 15 animals which had previously served to define the cells of origin of the normal entorhinal cortical projections (*8*).

We have recently described two subsystems of entorhinal cortical efferent nerves which differ on the basis of their topographic organization (*9*) and their cells of origin (*8*). One subsystem projects predominantly ipsilaterally to the dentate gyrus and regio inferior of the hippocampus proper (*9*), and originates from cells in layer II (probably stellate cells) of the entorhinal cortex (*8*). The second subsystem projects bilaterally to the regio superior of the hippocampus proper, and originates from cells (medium-sized pyramids) in layer III of the entorhinal region (*8*). Thus, injections of HRP which label the terminal fields of both subsystems result in bilateral labeling of cells in layer III, and predominantly ipsilateral labeling of cells in layer II (see Figs. 1 and 2). Rare, lightly labeled cells may be found in layer II contralateral to the injection, particularly in the medial entorhinal area (see Fig. 2, A and C), and these probably represent the cells of origin of the sparse, normal, crossed temporo-dentate projection (*8*), but in normal animals the major population of labeled cells in the entorhinal region contralateral to an injection are localized in layer III (see Fig. 2A).

Injections of HRP into the reinner-